Journal of Materials Chemistry

Cite this: *J. Mater. Chem.*, 2012, **22**, 24644

www.rsc.org/materials

PAPER

Extraction of resveratrol from *polygonum cuspidatum* with magnetic orcinol-imprinted poly(ethylene-*co*-vinyl alcohol) composite particles and their *in vitro* suppression of human osteogenic sarcoma (HOS) cell line

Mei-Hwa Lee,*[a] James L. Thomas,[b] Hsuan-Yun Wang,[a] Chih-Chun Chang,[c] Chuan-Chuan Lin[d] and Hung-Yin Lin*[c]

Received 30th June 2012, Accepted 1st October 2012
DOI: 10.1039/c2jm34244h

Resveratrol is thought to have many benefits to human health, including anti-oxidant and anti-cancer properties. It can be found in grapes and peanuts, but at low concentrations, and extraction from these sources involves enormous waste. A highly invasive and low-value plant, *polygonum cuspidatum* (PC) is a good source of resveratrol, provided an efficient method of extraction is developed. We report on the development of magnetic molecularly imprinted polymer particles that bind resveratrol, which could be used for the extraction of resveratrol from PC extracts. Magnetic nanoparticles were included in the synthesis to allow magnetic separations. Rather than using resveratrol itself as the imprinting template, a less expensive compound sharing important functional groups (orcinol) was used. The target recognition ability of the magnetic orcinol-imprinted poly(ethylene-*co*-vinyl alcohol) composite particles, MOIPs, was examined. Finally, *in vitro* suppression of human osteogenic sarcoma (HOS) cells by MOIPs, with and without resveratrol, was studied. Delivery of resveratrol *via* the imprinted polymer particles substantially increased the toxicity to these tumor cells.

1. Introduction

Although the claim that resveratrol extends the lifespan of human beings is still arguable, its cancer preventing, neuroprotective, anti-inflammatory, cardioprotective, anti-diabetic, and antiviral effects have frequently been noted in scientific literature. However, the poor systemic bioavailability of resveratrol, even at high oral doses, prevents bioeffective (such as cancer preventing) concentrations from being reached. The extraction and delivery of resveratrol may help to reduce the cost of its clinical use and increase its bio-effectiveness. Three major sources of resveratrol are grapes, peanuts and *polygonum cuspidatum* root, but the first two are foods, so recovery of resveratrol can result in considerable waste of nutritionally valuable material.[1,2] The antioxidant capacity of *polygonum cuspidatum* extract (PCE),[3,4] the anti-inflammatory activities of emodin and resveratrol, which inhibit NF-kB[5,6] and the mechanism of polydatin in shock treatment[7] have been described. The extraction of bioactive molecules from *polygonum cuspidatum* may be attractive not only because it can reduce the cost of purification, but also because products may be useful in anti-cancer therapies.

Molecularly imprinted polymers (MIPs) were originally developed for use in bioseparation, biosensing, bioimaging and drug delivery. Some conventional methods have been implemented to synthesize resveratrol-imprinted polymers, using resveratrol as the template; methacrylic acid, acrylamide,[8–10] styrene and 4-vinylpyridine[1,2] as the functional monomers; and ethylene glycol diamethacrylate as the cross-linking agent. One such method involves bulk polymerization by either ultraviolet or thermal methods, followed by crushing in a mortar to form 60–100 μm MIP particles and subsequent removal of the template by a mixture of methanol and acetic acid;[1,2,8] other imprinting methods have also been employed.[10–14] Resveratrol-imprinted polymeric thin films have also been coated on indium tin oxide electrodes for the electrochemical sensing of resveratrol.[9]

We have chosen to use a "proxy" template (orcinol) for resveratrol, for two reasons. Firstly, orcinol is considerably less expensive than resveratrol, and thus its potential applicability as a proxy template is of interest, particularly if scale-up to large quantities is desired. Secondly, we are primarily interested in the application of the MIP particles to the delivery of resveratrol to target cells. In this application, it may well be beneficial to avoid the tightest possible binding to the substrate, which could lead to nearly irreversible association and thereby reduce bioavailability.

[a]*Department of Materials Science and Engineering, I-Shou University, No1, Sec 1, Syuecheng Rd, Dashu District, Kaohsiung City 84001, Taiwan. E-mail: meihwalee@ntu.edu.tw; Fax: +886 (7) 657-8444; Tel: +886 (7) 657-7711 ext. 3128*
[b]*Department of Physics and Astronomy, University of New Mexico, Albuquerque, NM 87131, USA*
[c]*Department of Chemical and Materials Engineering, National University of Kaohsiung (NUK), 700, Kaohsiung University Rd., Nan-Tzu District, Kaohsiung 81148, Taiwan. E-mail: linhy@ntu.edu.tw; linhy@caa.columbia.edu; Tel: +886 (7) 591-9455; +886 (912) 178-751*
[d]*Department of Food Science, China Institute of Technology, Taipei 115, Taiwan*

Recently, MIPs have been combined with magnetic nanoparticles (MMIPs) to achieve bioseparations by active adsorption, followed by particle separation in a magnetic field gradient. Small biomolecules, such as tyrosine and phenylanine,[15] tryptophan,[16] tetracycline antibiotics,[17] atrazine,[18] biophenol A,[19–21] indole-3-acetic acid,[22] fluoroquinolone[23] and β-lactam antibiotics,[24] chlorogenic acid,[25] auxin,[26] theophylline,[27] β-agonists,[28] sildenafil, vardenafil[29] and 17β-estradiol,[30]have been used as target molecules in the synthesis of MMIPs.

In our earlier work, albumin- and urea-imprinted polymer nanoparticles were synthesized from poly(ethylene-*co*-vinyl alcohol), abbreviated as EVAL, *via* phase inversion,[31] with both target molecules and hydrophobic magnetic nanoparticles mixed within the polymer solution. The composite nanoparticles were used for the separation and sensing of template molecules (such as human serum albumin and urea) in real samples (such as urine). Here we report the synthesis of MMIPs for the purpose of binding resveratrol, but using a chemically and structurally similar analog, orcinol, as a template. The binding capacity, morphology and distribution of sizes of magnetic orcinol-imprinted poly(ethylene-*co*-ethylene alcohol) composite particles (MOIPs) were investigated by high-performance liquid chromatography (HPLC), dynamic light scattering (DLS) and transmission electron microscopy (TEM). Finally, the magnetic imprinted polymer particles were used for the purification of resveratrol from an extract of *polygonum cuspidatum* and their toxicity to cancer cells was evaluated *in vitro*.

2. Experimental section

2.1 Reagents and chemicals

Orcinol (5-methylresorcinol, 97%) (I), resveratrol (3,4′,5-trihydroxy-*trans*-stilbene, ≥99% GC grade) (II) and poly(ethylene-*co*-vinyl alcohol), EVAL, with ethylene 27, 32, 38 and 44 mol% (product # 414077, 414093, 414085, 414107) were from Sigma-Aldrich Co. (St Louis, MO). Dimethyl sulfoxide (DMSO, product # 161954) was purchased from Panreac (Barcelona, Spain) and used as the solvent to dissolve EVAL polymer particles in the concentration of 1 wt%. Iron(III) chloride 6-hydrate (97%) and iron(II) sulphate 7-hydrate (99.0%) were also from Panreac. Absolute ethyl alcohol was from J. T. Baker (ACS grade, NJ) and used for the removal of target molecules. All chemicals were used as received unless otherwise mentioned.

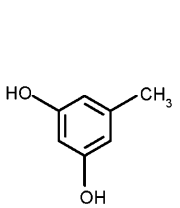

(I)

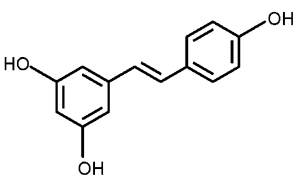

(II)

2.2 Formation of composite molecularly imprinted poly(ethylene-*co*-ethylene alcohol) particles

The synthesis of magnetic orcinol-imprinted and non-imprinted EVAL nanoparticles included four steps (as shown in Scheme 1). (1) Magnetic nanoparticles (MNP) were synthesised by the Massart method, which is simply co-precipitation of a mixture of iron(III) chloride 6-hydrate and iron(II) sulphate 7-hydrate by sodium hydroxide. This magnetite was mixed with oleic acid for better dispersion and repeatedly washed while adsorbed on a magnetic plate, and then freeze dried overnight. (2) Magnetic nanoparticles were added to the EVAL solution (EVAL/DMSO = 1 wt%) to a concentration of 20 mg mL^{-1}. The EVAL/magnetic particle solution was mixed with 0.1 mg mL^{-1} of orcinol. (3) The EVAL/magnetic particle solution was dispersed in 10 mL non-solvent solution[32] (deionized water/isopropanol = 2/3 in weight) for EVAL at 5 °C. (4) Template molecules and EVAL particles were removed from magnetic nanoparticles using a magnetic plate and washing with 1 mL various vol% of ethanol solution 3 min for 2 times and then deionized water 10 min for four times. All composite nanoparticles were equilibrated with deionized water overnight before use. The non-imprinted polymers (NIPs) were prepared identically, except that the template was omitted.

2.3 Kinetics of binding of the template or target to magnetic MIP and NIP composite particles

The rebinding of the template or target molecules to the molecularly imprinted or non-imprinted polymers was performed with 1 mL 0.01 mg mL^{-1} of orcinol or resveratrol solution, which was dissolved in the phosphate buffer saline (PBS). These solutions were added to 1 mg of polymer particles on a magnetic plate for 30 minutes. A UV/Vis spectrophotometer (Lambda 40, PerkinElmer, Wellesley MA) was then used to measure the concentration decrease in the stock solution, determined by absorption at 273 and 305 nm[8,11,12] for orcinol and resveratrol, respectively.

2.4 Size distribution and morphology of composite particles

Magnetic and orcinol-imprinted composite (magnetic/polymeric) nanoparticles were monitored by a particle sizer (90Plus, Brookhaven Instruments Co., New York). The measurement of the particle size distribution was based on DLS at 25 °C with 3 minutes duration data collection at the 90° detection angle. The average count rate of the background was 15 kcps and that of each measurement was between 20 and 500 kcps. The scattering laser power of this instrument is the standard 35 mW.

The morphology of magnetic poly(ethylene-*co*-vinyl alcohol) composite particles can be observed by using transmission electron microscopy (Hitachi, H-7500, Japan). Five μL of composite particles (DI water solution at 0.1 mg mL^{-1}) were placed on the lacey formvar/carbon, 200 mesh, copper grid (approx. hole size: 97 μm, 01800-F, Ted Pella, Inc., Redding, CA) for 5 min, and the excess liquid on the samples was wiped off with ADVANTEC (no.1, 125 mm, Toyo Roshi Kaisha, Ltd., Japan) filter paper, followed by air-drying at room temperature overnight.

2.5 Magnetization measurement of the magnetic molecularly imprinted EVAL composite nanoparticles

Superconducting quantum interference devices (SQUID) are very sensitive magnetometers used to measure extremely small magnetic fields, based on superconducting loops containing Josephson junctions. The magnetic nanoparticles and

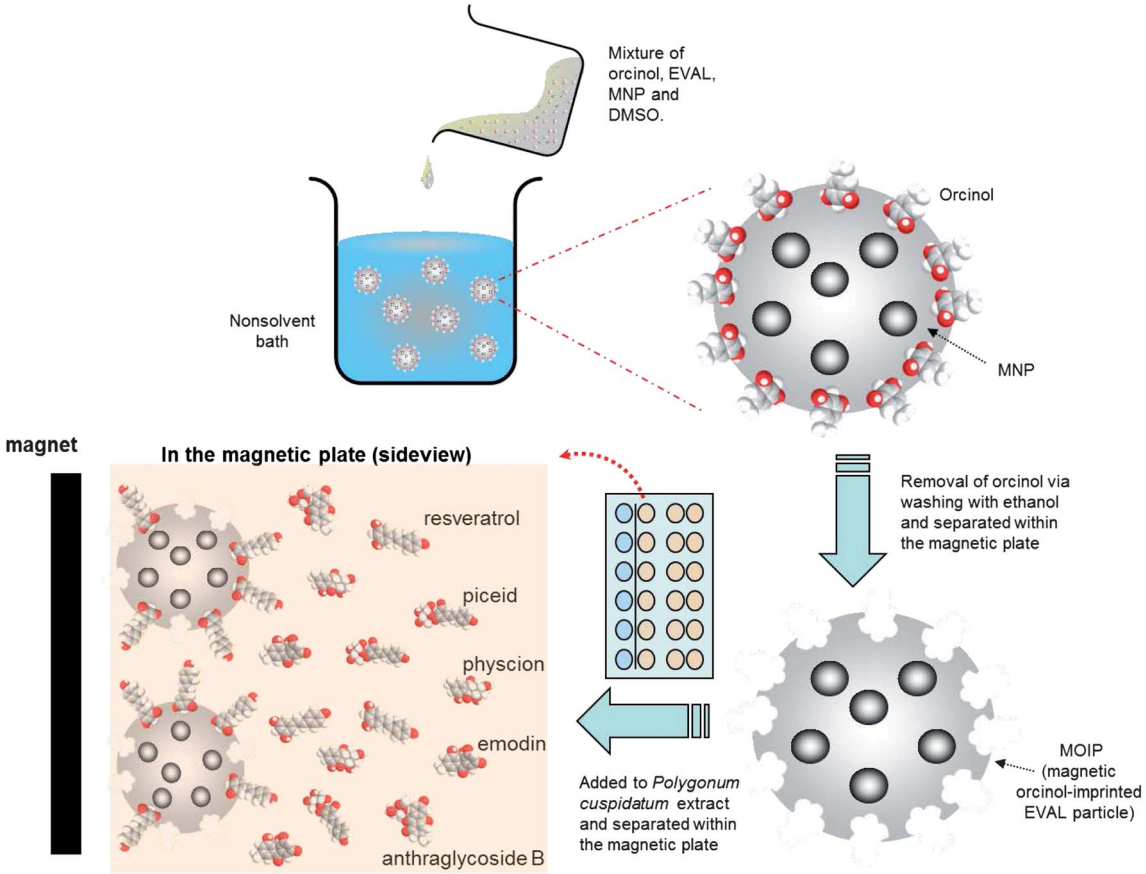

Scheme 1 The separation of target molecules using MOIP composite particles from the *polygonum cuspidatum* extract.

orcinol-imprinted magnetic EVAL composite nanoparticles before and after removal of template were freeze dried and their magnetization monitored with a magnetic property measurement system (MPMS XL-7, Quantum Design, San Diego, CA) at 298 K in ±15 000 Gauss.

2.6 Adsorption and recovery of the resveratrol from the *polygonum cuspidatum* extract by the composite particles

Polygonum cuspidatum powder (10 g) was dissolved in 40 mL ethanol (99%, HPLC grade), sonicated for 20 min and left stationary for 20 min 3 times and then filtered with ADVANTEC (no.1, 125 mm, Toyo Roshi Kaisha, Ltd., Japan) filter paper. The resultant solution was passed through a 0.45 μm filter and then subjected to HPLC for analysis of the four major components in PC. The separation was performed on a Cosmosil 5C18 MS column (50 μm, 25 cm × 4.6 mm I.D., Nacalai Tesque, Kyoto, Japan). The sample (20 μL) was eluted with a mobile phase composed of 0.1% H_3PO_4 (A) and acetonitrile (B) and a gradient profile as follows: 0–5 min, from 90% A, 10% B to 70% A, 30% B; 5–20 min, from 70% A, 30% B to 60% A, 40% B; 20–40 min, from 60% A, 40% B to 10% A, 90% B; 40–45 min, from 10% A, 90% B to 5% A, 95% B. The flow rate and detection wavelength were set to be 1.0 mL min^{-1} and 280 nm, respectively. These flow parameters are in accord with prior work.[33] It is necessary to perform a HPLC profile within 50 min for analyzing natural products, since a well-designed mobile phase gradient is required to separate all the components in the extract to make sure no co-eluents contaminate the analyzed target peaks. The standard curves of the four components in 50% ethanol ranging from 0.1 to 0.001 mg mL^{-1} were used for calculation. The retention time for the four phytochemicals were 8.91, 12.8, 33.7 and 41.1 min for polydatin, resveratrol, emodin and physcion, respectively. Emodin, a major anthraquinone in PC, has been reported to possess chemopreventive, antitumor, and estrogenic activities.[34,35] Physcion was previously found to have no cytotoxic activity on some cancer cell lines such as K562, HeLa, Calu-1, Wish and Raji.[36] However, polydatin was shown to elicit numerous biological effects through its anti-inflammatory and anti-oxidant properties.[37]

2.7 Cytotoxicity test of HOS cells with magnetic molecularly imprinted EVAL composite nanoparticles

The CCk-8 test (Sigma-Aldrich Chemical Co., Japan) is used as a rapid and sensitive method for screening toxicity of washed MOIPs (wMOIPs), resveratrol bound-MOIPs (Res.-MOIPs) and PC-extract-MOIPs (PCE-MOIPs) on HOS cells. About 2×10^3 HOS cells were added to each well of the 96-well culture plate (Nalge Nunc International, Rochester, NY) and incubated (37 °C and 5% CO_2) for 24 h. One mL of 10 × PCE or 1 μg mL^{-1} resveratrol solution (10 vol% ethanol) was used for a 30 min adsorption by 1 mg of MOIPs. Thirty microliters of the one mL of those particles were added to each well containing cells and

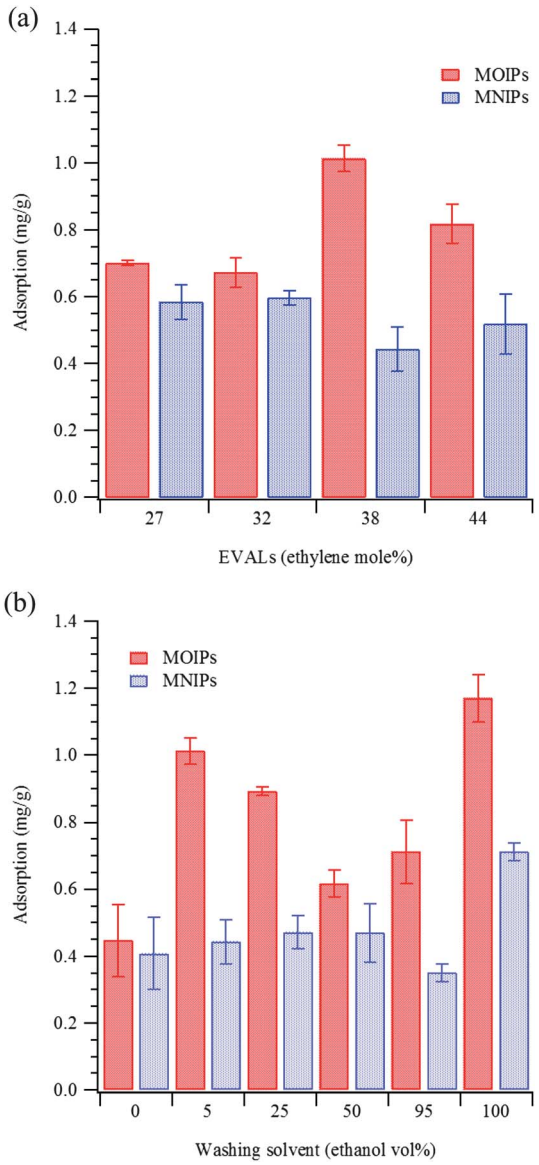

Fig. 1 The adsorption of orcinol onto magnetic orcinol- and non-imprinted poly(ethylene-*co*-vinyl alcohol) composite particles (a) containing various ethylene mol%, and (b) template removal with different vol% ethanol solutions.

incubated for another 24 h. Particles were removed from wells before ELISA measurements. Ten microliters of CCk-8 solution was added to each well and incubated for 3 h. Absorption (I_{450nm}) at 450 nm was measured with an ELISA reader Expert 96 (ASYS Hi-tech., Eugendorf, Austria), and the reference absorption (I_{650nm}, to account for turbidity and scattering) was obtained at the wavelength of 650 nm. The cellular viability (%) was then calculated from the ratio of effective absorption ($I_{450nm} - I_{650nm}$) of experimental cells to controls.

2.8 Cellular nuclear staining

6-well culture plates were used for the DAPI staining. Two mL modified Eagle medium (MEM) was added to each well (Nunc, Roskilde, Denmark), then 100 μL containing 2×10^4 HOS cells were added into each well. The 6-well culture plate was incubated at 37 °C and 5% CO_2 for 24 h. After incubation, 1 mg MOIPs, Res.-MOIPs or PCE-MOIPs were added into each well, followed by incubation at 37 °C and 5% CO_2 for 24 h. MEM was removed and then cells were washed with 2 mL Phosphate Buffered Saline (PBS) three times in each well. Cells were fixed with 2 mL per well of 3.7% Para Formaldehyde (PFA) for 10 min. After removing PFA, cells were washed with 2 mL per well PBS three times. 2 mL per well 0.1% Triton-X-100/PBS for 5 minutes was used to permeabilize cells. This solution was removed, and then 2 mL per well PBS was added and cells were washed three times. 2 mL per well 7.5% bovine serum albumin in PBS was added and incubated at 4 °C for 1 h. The bovine serum albumin solution was removed, and then 2 mL per well PBS was added and cells washed three times. 2 mL of DAPI (concentration of 10 ng mL^{-1} in PBS) was added into each well to stain cells for 5 minutes. DAPI was removed in each well, and then 2 mL per well PBS was added and cells washed three times. The 6-well culture plate was placed in the dark at room temperature till until each well was dry. Finally, the morphologies of cell nuclei were obtained using an inverted fluorescence microscope (CKX41, Olympus, Melville, NY).

3. Results and discussion

The epitope recognition of proteins, in which only one or two functional groups are recognized, is the basis of most ligand-receptor binding. We endeavoured to exploit this concept in the synthesis of MIPs in this work, by using a small analog of resveratrol as the template. This approach can be advantageous in improving the template solubility in the polymer/solvent mixture, and can reduce the need for valuable or toxic template molecules.

Numerous factors influence the rebinding capacity of MIPs, such as the composition of the functional monomers and

Table 1 Rebinding of template molecules to the magnetic molecularly imprinted and non-imprinted poly(ethylene-*co*-ethylene alcohol) and their imprinting effectiveness using different ethylene mol% EVALs[a]

EVAL (ethylene mol%)	Orcinol adsorption/mg g^{-1}			Resveratrol adsorption/mg g^{-1}		
	MOIPs	MNIPs	IF	MOIPs	MNIPs	IF
27	0.701 ± 0.008	0.585 ± 0.052	1.20	0.914 ± 0.004	0.455 ± 0.024	2.01
32	0.672 ± 0.045	0.597 ± 0.022	1.13	0.579 ± 0.043	0.506 ± 0.0017	1.14
38	1.013 ± 0.039	0.443 ± 0.066	2.29	1.643 ± 0.098	0.559 ± 0.123	2.94
44	0.818 ± 0.057	0.519 ± 0.090	1.58	0.865 ± 0.008	0.629 ± 0.006	1.37

[a] MOIPs: magnetic orcinol-imprinted polymers; MNIPs: magnetic non-imprinted polymers; IF: imprinting effectiveness.

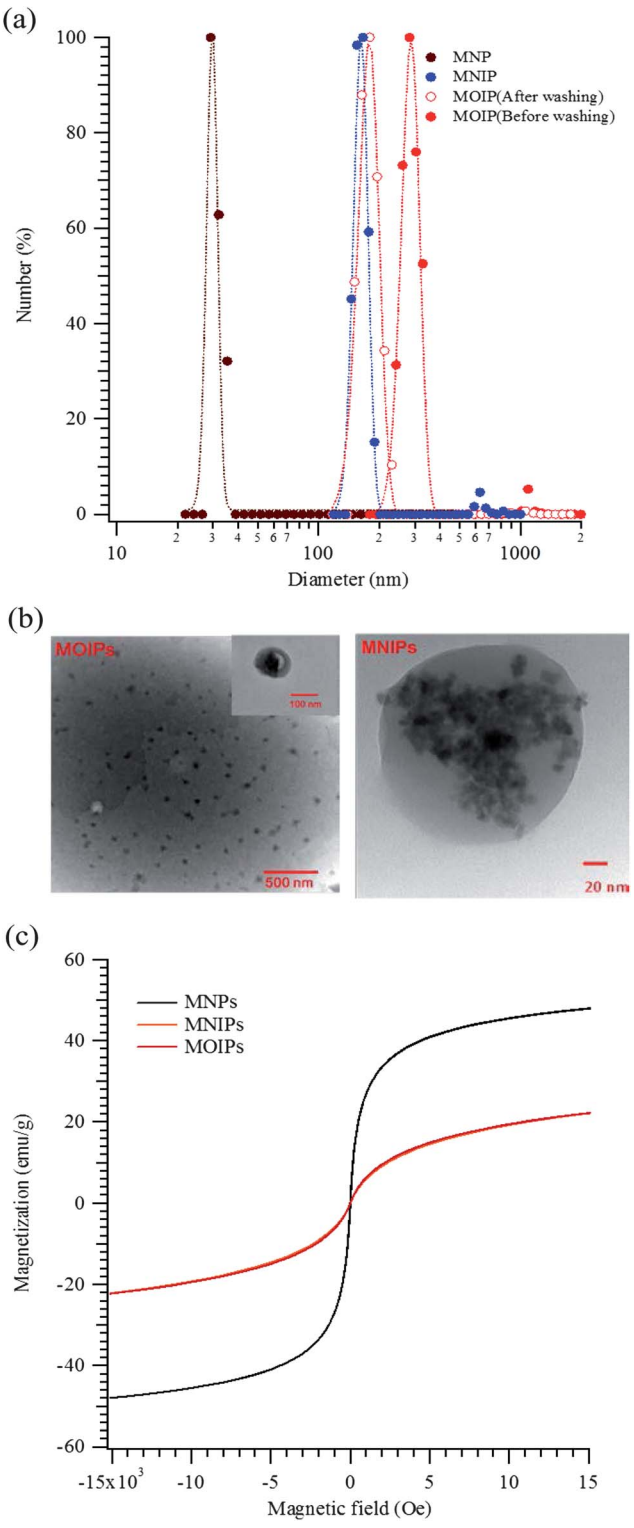

Fig. 2 (a) The particle size distribution of magnetic, non- and orcinol-imprinted EVAL composite particles after and before template removal. (b) The TEM images of the magnetic orcinol- and non-imprinted EVAL composite particles. (c) SQUID magnetization measurement of magnetic particles and orcinol-imprinted magnetic EVAL nanoparticles imprinted with different concentrations of orcinol.

templates. Conventionally, MIPs have been thought to create surface area (for example by making the particle structure porous), increasing the binding capacities for target molecules. Fig. 1(a) presents the adsorption of orcinol on the MOIPs and magnetic non-imprinted polymers (MNIPs) made with various ethylene ratios of EVAL. The capacities of MNIPs for orcinol were approximately 0.49 ± 0.07–0.59 ± 0.05 mg g^{-1} of particles. The small variation of capacity with composition suggests that the surface adsorption is non-specific. The readsorption of orcinol on the MOIPs is as high as 1.03 ± 0.06 mg g^{-1} of particles, which was optimized at 38 mol% ethylene. The imprinting effectiveness is defined as the ratio of the amount of orcinol bound to MIPs to that of NIPs. As indicated in Table 1, the imprinting effectiveness of MOIPs is between 1.13 and 2.29, depending on ethylene content.

In the above experiments, ethanol/water solutions (10 vol% ethanol) were used to wash the template from the MOIPs prior to rebinding measurements. Changing the fraction of ethanol in the washing solution has a large effect on the rebinding of orcinol, as shown in Fig. 1(b). With no ethanol, there is no specific rebinding (no difference between MOIPs and MNIPs), most likely because the water wash is unable to free the template molecules. Modest concentrations (5, 25 vol%) of ethanol are effective, but readsorption falls at 50 vol%. This may occur because of swelling and reorganization of binding pockets in this washing solution. Interestingly, the great swelling that was caused by ethanol[38] also increased the adsorption of orcinol on both MOIPs and MNIPs. The lowest effective ethanol concentation, 5 vol%, was used in subsequent washings, as this gave the best specificity.

Fig. 2 displays the distribution of sizes and the morphologies of the MNPs, and MNIPs and MOIPs. In Fig. 2(a), the mean diameters of these particles determined by dynamic light scattering were 29, 166, and 282 (before wash) or 179 nm (after wash; 5 vol% ethanol) respectively. The larger mean size of MOIPs before washing may reflect some aggregation in the presence of orcinol. Fig. 2(b) shows an electron micrograph of a few MOIP composite particles and a single MNIP composite particle. The sizes of MNIPs and MOIPs were measured to be 163 and 171 nm, which are very close to those measured by DLS, as presented in Fig. 2(a). The electron micrograph shows that the mean size of the magnetic nanoparticles is rather smaller than that estimated using DLS and in addition, the magnetic particles are not uniformly dispersed in the EVAL composite particles. Fig. 2(c) shows the magnetization of the magnetic nanoparticles and the synthesized composite particles. The superparamagnetic property of the magnetic nanoparticles was retained in the composite particles. The MOIPs and MNIPs showed a magnetization reduced by about 53% (from 47.9 to 22.2 emu g^{-1} under a 15 000 Gauss magnetic field), compared to the MNPs alone.

Fig. 3(a) and (b) present the binding of orcinol and resveratrol to the MNIPs and MOIPs, as a function of binding time. The molecular weights of orcinol and resveratrol are 124.13 and 228.24 g mol^{-1}, respectively. Hence, the amounts of orcinol and resveratrol that are re-bound to MOIPs are 1.01 and 1.4 mg g^{-1} of particles or approximately 8.14 and 6.13 μmol g^{-1} of particles.

Fig. 3(c) shows the ability of MOIPs synthesized using different concentrations of template to recognize template (orcinol) and target (resveratrol) molecules. The adsorption amount of orcinol was highest when 0.1 mg mL^{-1} of orcinol was

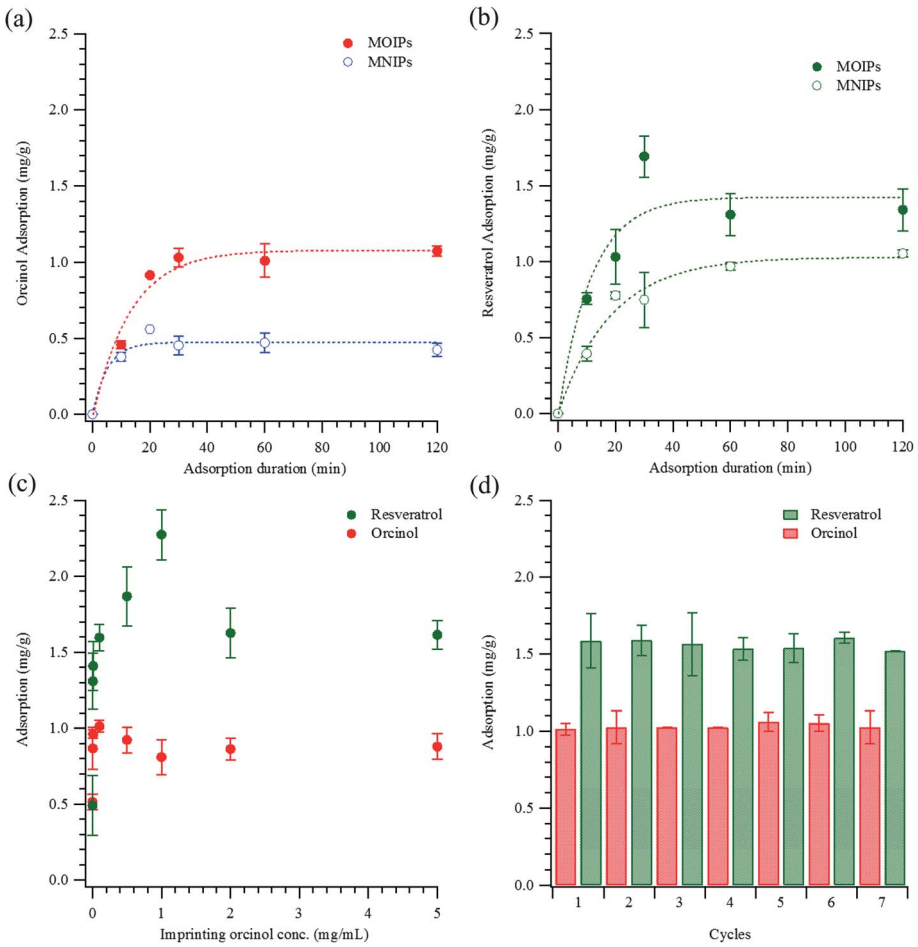

Fig. 3 The adsorption of (a) orcinol and (b) resveratrol to the magnetic orcinol and non-imprinted EVAL composite particles, as a function of binding time (duration). (c) The binding as a function of the imprinting orcinol concentration. (d) The reusability of the magnetic orcinol-imprinted EVAL composite particles. Rebinding orcinol and resveratrol concentration and duration were 0.05 mg mL^{-1} and 30 min, respectively, for (c) and (d).

used for imprinting; however, the adsorption of resveratrol was 2.3 mg or 10.08 μmol g^{-1} of particles when 1 mg mL^{-1} of oricinol was used for imprinting. An imprinting concentration of greater than 2 mg mL^{-1} of orcinol may have created a rougher surface than a lower concentration, reducing the adsorption of the larger target resveratrol molecule but not the template orcinol molecule.

The optimal adsorption conditions for MOIPs were obtained using 0.1 mg mL^{-1} orcinol for imprinting, an adsorption duration of 30 min, and removal of the template using 5 vol% of ethanol, and adsorption template and target concentrations of 0.01 mg mL^{-1}. At least seven readsorption cycles of the MOIPs were conducted, as shown in Fig. 3(d); the small reduction of the readsorption ability may have been caused not only by the loss of particles but also by the swelling of the MIP structure during the template removal.

PCE was then used to examine the recognition of polyphenols (such as polydatin, resveratrol, emodin and physcion). In Table 2, the concentrations of polydatin, resveratrol, emodin and physcion in the stock PCE are 495 ± 14, 444 ± 16, 314 ± 5 and 1090 ± 36 μg mL^{-1}, respectively. The fraction of resveratrol removed from PCE (measured by HPLC analysis) reaches 37.8%

Table 2 The adsorption and recovery of components in the *polygonum cuspidatum* extract by magnetic orcinol- and non-imprinted EVAL composite particles

Bioactive molecules	Extract of *polygonum cuspidatum*/μg mL^{-1}	Adsorption by magnetic composite particles/μg mL^{-1}		Effectiveness	Recovered from MOIPs/μg mL^{-1}
		MOIPs	MNIPs		
Polydatin	495 ± 14	27 ± 12	19 ± 2	1.42	12 ± 1
Resveratrol	444 ± 16	168 ± 60	40 ± 15	4.23	99 ± 6
Emodin	314 ± 5	21 ± 13	11 ± 2	2.01	11 ± 2
Physcion	1090 ± 36	83 ± 34	52 ± 2	1.58	41 ± 3

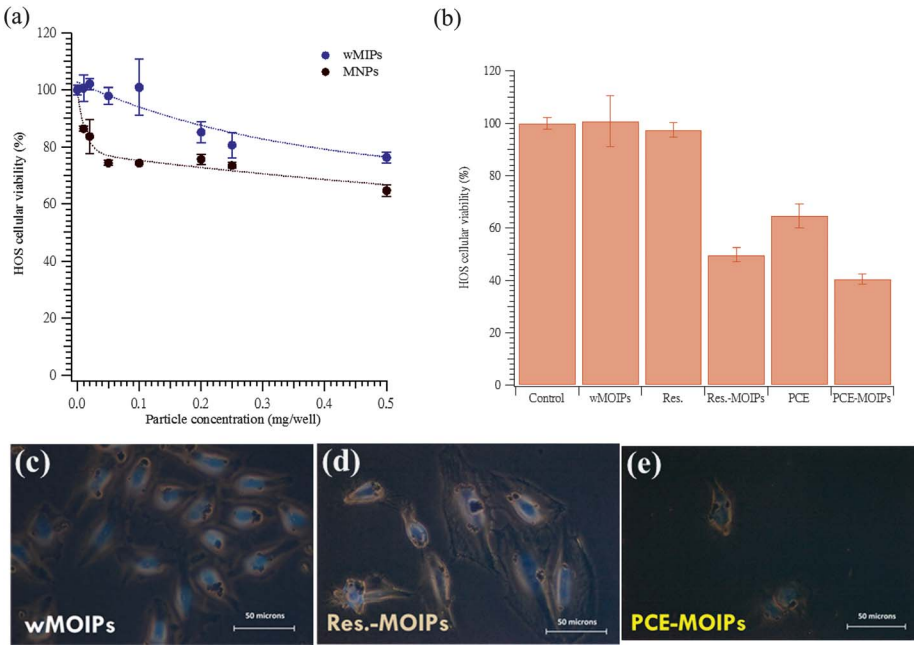

Fig. 4 (a) The cellular viability of HOS cells after treatment with different concentrations of wMOIPs and MNPs. (b) The cellular viability of HOS cells treated with wMOIPs, resveratrol, Res.-MOIPs, PCE and PCE-MOIPs, where the dosage was 0.1 mg particles per well and the resveratrol concentration applied was 0.01 mg mL^{-1} in all cases. Fluorescence images of DAPI-stained fixed cells treated with (c) wMOIPs, (d) Res.-MOIPs and (e) PCE-MOIPs.

when only 1 mg of MOIPs was used. For other potentially interfering compounds, this value falls to less than 8%. The binding capacity for resveratrol and selectivity *vs.* polydatin were 168 ± 60 mg g^{-1} and 6.26. These figures of merit are actually considerably better than most previously reported with resveratrol-imprinted MIPs, *e.g.* 30.16 mg g^{-1} with a selectivity of 1.18.[8] In a different study using core–shell imprinted microspheres an absorption of 3.22 mg g^{-1} and a separation factor (*i.e.* ratio of retention time difference) 2.61 were found.[12] A third study with resveratrol-imprinted particles used in HPLC reported a binding capacity of only 0.064 mg g^{-1}, and a purification purity of 80.1% (implying an effectiveness against emodin, the major competitive binder, of at least 4).[11] Other core–shell molecularly imprinted microspheres showed a resveratrol absorption of 13.80 mg g^{-1}.[14] For our particles, the imprinting effectiveness (ratio of amount bound to imprinted *vs.* non-imprinted particles) using PC extract reached 4.23 for resveratrol, but was less than 2.01 for the other three molecules.

Fig. 4(a) plots the effects of the amount of MNPs and wMOIPs on cell viability. The cell toxicities were approximately 60.9 ± 5.4 when the mass of MNPs (black symbol) was 0.1–0.5 mg per well in 96 cell plates. The cellular viability was 100% when the mass of wMOIPs was less than 0.1 mg per well (blue symbols). These results clearly reveal that 0.1–0.5 mg MNPs per well are toxic to HOS cells, but 0.1 mg per well wMOIPs do not harm these cells. Fig. 4(b) displays the cellular viabilities of HOS cells in the presence of wMOIPs, resveratrol solution (Res.), Res.-MOIPs, PCE and PCE-MOIPs. The masses of wMOIPs, Res.-MOIPs and PCE-MOIPs were all 0.1 mg per well (*ca.* 0.435 mg mL^{-1}), to prevent toxicity from the composite nanoparticles themselves. The concentration of resveratrol was 0.13 μg mL^{-1} in each well except for controls. HOS cell viability was ~100% when they were cultured with wMOIPs or Res. *separately*, as shown in Fig. 4(b). A comparison of two sets of Res. and Res.-MOIPs/PCE and PCE-MOIPs revealed that the Res.-MOIPs and PCE-MOIPs were more toxic than Res. solution and *polygonum cuspidatum* extract, respectively. These results show a synergistic toxicity effect of the MOIPs and the resveratrol or PCE; this effect may arise from more effective delivery of Res. or PCE to cells when bound to MOIPs.

Fig. 4(c)–(e) display images of DAPI (4′,6-diamidino-2-phenylindole)-stained HOS cells treated with wMOIPs, Res.-MOIPs and PCE-MOIPs (from left to right), respectively. The DAPI images, obtained using a fluorescence microscope, show that the number of cells declines from Fig. 4(c)–(e). This finding demonstrates that Res.-MOIPs and PCE-MOIPs cause more cellular lysis than wMOIPs. Additionally, PCE-MOIPs were even more toxic than Res.-MOIPs, as shown in Fig. 4(d) and (e).

4. Conclusions

In this investigation, poly(ethylene-*co*-ethylene alcohol), EVAL, was molecularly imprinted with orcinol (which may be considered an "epitope" of resveratrol) *via* non-solvent precipitation processing. Magnetic nanoparticles were included to aid in separations. The magnetic orcinol-imprinted polymer particles (MOIPs) were able to absorb resveratrol from pure solutions but also from *polygonum cuspidatum* extract (PCE), which is an economically attractive source for this medically important natural product. Other polyphenols were also absorbed, but mostly non-specifically. Finally, we observed a synergistic toxicity of MOIPs and resveratrol (or PCE) in the killing of cancer cells *in vitro*, possibly caused by enhanced delivery of these compounds to cells mediated by the

nanoparticles. This enhanced toxicity is an important result in and of itself; however the mechanisms clearly require further study.

Acknowledgements

We appreciate financial support from the National Science Council of ROC under Contract no. NSC101-2320-B-214-006-, NSC 100-2314-B-390-001-MY3 and NSC 99-2221-E-214-033-.

References

1 L. J. Schwarz, B. Danylec, Y. Yang, S. J. Harris, R. I. Boysen and M. T. W. Hearn, *J. Agric. Food Chem.*, 2011, **59**, 3539–3543.
2 L. J. Schwarz, B. Danylec, S. J. Harris, R. I. Boysen and M. T. W. Hearn, *J. Chromatogr., A*, 2011, **1218**, 2189–2195.
3 H. Masaki, S. Sakaki, T. Atsumi and H. Sakurai, *Biol. Pharm. Bull.*, 1995, **18**, 162–166.
4 C.-Y. Hsu, Y.-P. Chan and J. Chang, *Biol. Res.*, 2007, **40**, 13–21.
5 A. Kumar, S. Dhawan and B. B. Aggarwal, *Oncogene*, 1998, **17**, 913–918.
6 S. K. Manna, A. Mukhopadhyay and B. B. Aggarwal, *J. Immunol.*, 2000, **164**, 6509–6519.
7 K.-s. Zhao, C. Jin, X. Huang, J. Liu, W. S. Yan, Q. Huang and W. Kan, *Clin. Hemorheol. Microcirc.*, 2003, **29**, 211–217.
8 H. Cao, J. Xiao and M. Xu, *Macromol. Res.*, 2006, **14**, 324–330.
9 H. Y. Xiang and W. G. Li, *Electroanalysis*, 2009, **21**, 1207–1210.
10 H.-Y. Xiang, C.-S. Zhou, S.-A. Zhong and Q.-F. Lei, *Chin. J. Appl. Chem.*, 2005, **22**, 739–743.
11 X. Zhuang, X. Dong, S. Ma and T. Zhang, *J. Chromatogr. Sci.*, 2008, **46**, 739–742.
12 Z. Zhang, L. Liu, H. Li and S. Yao, *Appl. Surf. Sci.*, 2009, **255**, 9327–9332.
13 M.-h. Hong, Y.-t. Chen, J. Wang, X.-l. Wang and L.-s. Cai, *Nat. Prod. Res. Dev.*, 2010, **22**, 559–563.
14 M.-L. Zhang, Z.-H. Zhang, L. Liu, L.-J. Zhang and L.-H. Nie, *Chin. J. Anal. Chem.*, 2010, **38**, 129–132.
15 S. Lu, G. Cheng and X. Pang, *J. Appl. Polym. Sci.*, 2003, **89**, 3790–3796.
16 S. Lu, G. Cheng, H. Zhang and X. Pang, *J. Appl. Polym. Sci.*, 2006, **99**, 3241–3250.
17 L. Chen, J. Liu, Q. Zeng, H. Wang, A. Yu, H. Zhang and L. Ding, *J. Chromatogr., A*, 2009, **1216**, 3710–3719.
18 Y. Hu, R. Liu, Y. Zhang and G. Li, *Talanta*, 2009, **79**, 576–582.
19 Y. Ji, J. Yin, Z. Xu, C. Zhao, H. Huang, H. Zhang and C. Wang, *Anal. Bioanal. Chem.*, 2009, **395**, 1125–1133.
20 W. Guo, W. Hu, J. Pan, H. Zhou, W. Guan, X. Wang, J. Dai and L. Xu, *Chem. Eng. J.*, 2011, **171**, 603–611.
21 J. Pan, L. Xu, J. Dai, X. Li, H. Hang, P. Huo, C. Li and Y. Yan, *Chem. Eng. J.*, 2011, **174**, 68–75.
22 Y. Zhang, Y. Li, Y. Hu, G. Li and Y. Chen, *J. Chromatogr., A*, 2010, **1217**, 7337–7344.
23 L. Chen, X. Zhang, Y. Xu, X. Du, X. Sun, L. Sun, H. Wang, Q. Zhao, A. Yu, H. Zhang and L. Ding, *Anal. Chim. Acta*, 2010, **662**, 31–38.
24 X. Zhang, L. Chen, Y. Xu, H. Wang, Q. Zeng, Q. Zhao, N. Ren and L. Ding, *J. Chromatogr., B: Anal. Technol. Biomed. Life Sci.*, 2010, **878**, 3421–3426.
25 X.-h. Gu, R. Xu, G.-l. Yuan, H. Lu, B.-r. Gu and H.-p. Xie, *Anal. Chim. Acta*, 2010, **675**, 64–70.
26 Y. Hu, Y. Li, Y. Zhang, G. Li and Y. Chen, *Anal. Bioanal. Chem.*, 2011, **399**, 3367–3374.
27 X. Luo, F. Deng, S. Luo, X. Tu and L. Yang, *J. Appl. Polym. Sci.*, 2011, **121**, 1930–1937.
28 Y. Hu, Y. Li, R. Liu, W. Tan and G. Li, *Talanta*, 2011, **84**, 462–470.
29 M. Ding, X. Wu, L. Yuan, S. Wang, Y. Li, R. Wang, T. Wen, S. Du and X. Zhou, *J. Hazard. Mater.*, 2011, **191**, 177–183.
30 S. Wang, Y. Li, M. Ding, X. Wu, J. Xu, R. Wang, T. Wen, W. Huang, P. Zhou, K. Ma, X. Zhou and S. Du, *J. Chromatogr., B: Anal. Technol. Biomed. Life Sci.*, 2011, **879**, 2595–2600.
31 M.-H. Lee, J. L. Thomas, M.-H. Ho, C. Yuan and H.-Y. Lin, *ACS Appl. Mater. Interfaces*, 2010, **2**, 1729–1736.
32 T.-H. Young, L.-P. Cheng, C.-C. Hsieh and L.-W. Chen, *Macromolecules*, 1998, **31**, 1229–1235.
33 M.-H. Lee, L. Kao and C.-C. Lin, *J. Agric. Food Chem.*, 2011, **59**, 9135–9141.
34 H. Matsuda, H. Shimoda, T. Morikawa and M. Yoshikawa, *Bioorg. Med. Chem. Lett.*, 2001, **11**, 1839–1842.
35 G. Srinivas, S. Babykutty, P. P. Sathiadevan and P. Srinivas, *Med. Res. Rev.*, 2007, **27**, 591–608.
36 Y.-C. Kuo, C.-M. Sun, J.-C. Ou and W.-J. Tsai, *Life Sci.*, 1997, **61**, 2335–2344.
37 H. Ji, X. Zhang, Y. Du, H. Liu, S. Li and L. Li, *Brain Res. Bull.*, 2012, **87**, 50–59.
38 W.-Y. Chuang, T.-H. Young, D.-M. Wang, R.-L. Luo and Y.-M. Sun, *Polymer*, 2000, **41**, 8339–8347.